Available online at www.sciencedirect.com
SCIENCE DIRECT®
ELSEVIER
Colloids and Surfaces A: Physicochem. Eng. Aspects 284–285 (2006) 250–253
COLLOIDS AND SURFACES A
www.elsevier.com/locate/colsurfa

Simple preparation of hemispherical polystyrene particles

Takeshi Higuchi [a], Hiroshi Yabu [b,c], Masatsugu Shimomura [b,c,d,*]

[a] *Graduate School of Science, Hokkaido University, N10W8, Kita-ku, Sapporo, Hokkaido 060-0810, Japan*
[b] *Nanotechnology Research Center, Research Institute for Electronic Science, Hokkaido University, N21W10, Kita-ku, Sapporo, Hokkaido 001-0021, Japan*
[c] *Frontier Research System, The Institute of Physical and Chemical Research (RIKEN), 2-1 Hirosawa, Wako, Saitama 351-0198, Japan*
[d] *Core Research for Evolutional Science and Technology (CREST), Japan Science and Technology Agency (JST), 4-1-8 Honcho, Kawaguchi, Saitama 332-0012, Japan*

Received 1 August 2005; received in revised form 17 October 2005; accepted 28 October 2005
Available online 4 January 2006

Abstract

We show the simple preparation of the hemispherical polymer particles. Submicron sized hemispherical polystyrene particles were prepared by adding a poor solvent (water) into a tetrahydrofran (THF) solution of polystyrene and following evaporation of THF. When the concentration of the polymer solution was higher than 0.4 g/L, spherical particles were formed. On the other hand, the hemispherical nano-particles were formed in the case of the dilute solution whose concentration was lower than 0.2 g/L. Turbidity change of the polymer solution due to THF evaporation starts from the surface of the solution. The light scattering experiment suggests that the hemispherical nano-particles were formed by precipitation at the air/solution interface.

Keywords: Polymer particles; Self-organization; Polystyrene; Hemispherical particles

1. Introduction

Polymer nano-particles can be used for versatile applications in the fields of photonics [1], electronics [2] and biotechnology [3]. Morphology of particles is one of the significant factors of determining their optical, interfacial and thermal properties of the particles themselves and their dispersions. There are many reports [4] about preparation of polymer nano-particles by conventional methods including milling bulk materials, emulsion polymerization, reprecipitation [5] and so on. Large varieties of particle morphology, spherical, hemispherical, disk and doughnut shapes have been reported [4].

Recently, we found that nano-particles can be prepared by evaporating a good solvent after addition of a poor solvent into a polymer solution (Fig. 1) [6–8]. In the commonly used reprecipitation process, polymer particles are immediately precipitated when a small amount of polymer solution is dropped into a large amount of poor solvent. In contrast, in our method, a small amount of poor solvent is slowly dropped into a polymer solution. Gradually, evaporation of the good solvent at room temperature causes precipitation of the polymer solute as fine particles. By using this method, nano-particles can be prepared from variety of polymers (e.g., engineering plastics, biodegradable polymers and electro-conductive polymers, etc.). The diameter of particles can be controlled by changing the concentration of the solution, the mixing ratio of the good solvent and the poor solvent, respectively. In the case of polystyrene particles, their size were controlled from several tens nm to several tens μm [6]. And shape of particles is basically sphere.

In this report, we found that the hemispherical polystyrene nano-particles are formed from THF solutions when the concentration of the polymer solution is lower than 0.2 g/L.

2. Experimental details

Polystyrenes with narrow molecular weight distribution (Mn: 10,5300, Mw: 11,0300, Mw/Mn: 1.05) were purchased from Scientific Polymer Products Inc., USA. Polystyrene was dissolved in THF, to prepare 1.0–0.02 g/L solutions. Two milliliters of Milli-Q water (Millipore Co., USA) was slowly added into 1 mL of the polymer solution with stirring. After 2 min stirring, the solution was stand at room temperature for complete

* Corresponding author. Tel.: +81 11 706 9368; fax: +81 11 706 9363.
E-mail address: shimo@poly.es.hokudai.ac.jp (M. Shimomura).

0927-7757/$ – see front matter © 2005 Elsevier B.V. All rights reserved.
doi:10.1016/j.colsurfa.2005.10.042

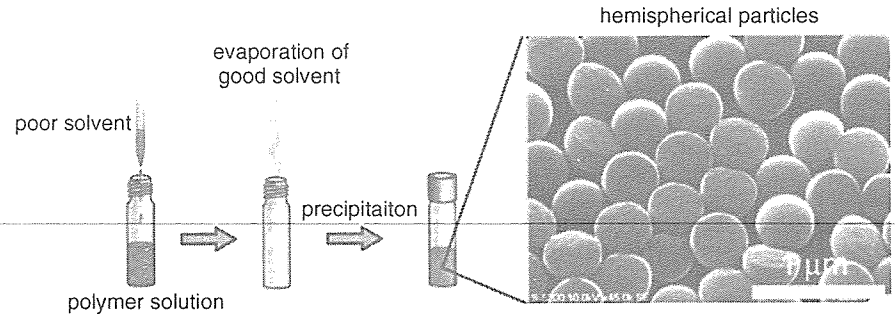

Fig. 1. Preparation method of hemispherical particles.

evaporation of THF. Diameters of the particles were measured by dynamic light scattering (DLS, ELS-8000 and FDLS-3000, Otsuka Electronics, Co., Ltd., Japan). Morphologies of the particles were observed by a scanning electron microscope (SEM, S-5200, Hitachi, Japan). For SEM observation, 100 μL of the water dispersions of the particles was dropped on to freshly cleaved mica substrates, and then spattered by Osmium (Os) after drying. Turbidity change of the polymer solution during the THF evaporation was measured. Time courses of the scattering intensities of 670 nm laser light at the upper region (3 mm from the surface of the solution) and the bottom region (1 mm from the bottom of the solution) of solution were measured at room temperature, respectively.

3. Results and discussion

The micron-scale spherical shaped particles with narrow size distribution were formed when the concentration of the polymer solution was higher than 0.4 g/L (Fig. 2, dark gray region). When the concentration of the solution was lower than 0.2 g/L (Fig. 2, white region), hemispherical shaped particles, which diameter was less than 1 μm, were formed. When the concentration of solution was in the range from 0.2 to 0.4 g/L (Fig. 2, gray region), both hemispherical and spherical shaped particles were observed. The particle shape was gradually changed from spherical to hemispherical by decreasing the concentration of the solution.

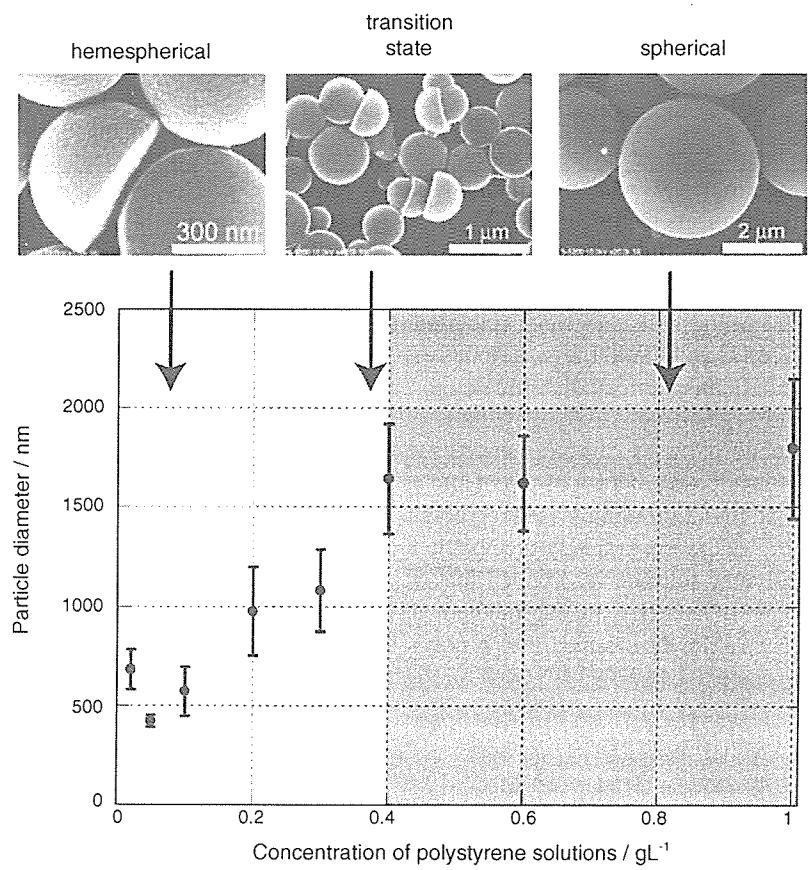

Fig. 2. Plot of mean particle diameters vs. concentration of polymer solutions. SEM image of the spherical and hemispherical polystyrene particles.

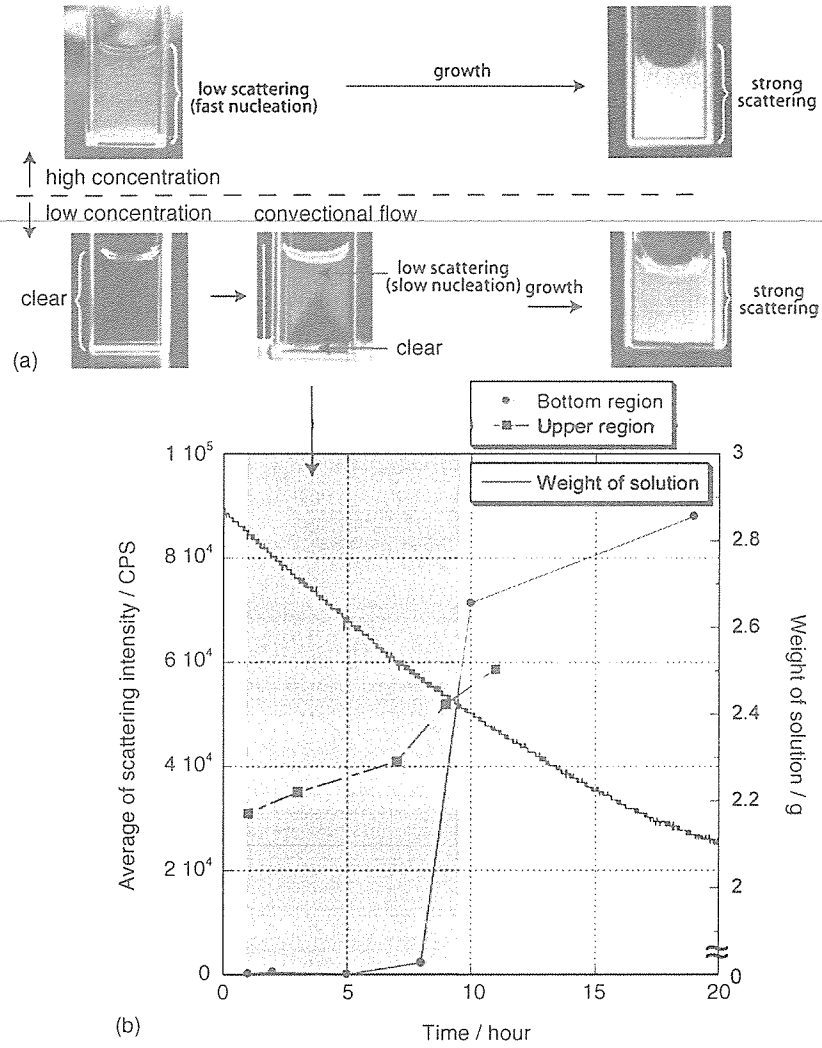

Fig. 3. (a) Turbidity change of the polymer solution during THF evaporation. (b) Time courses of the light scattering intensity at the bottom and upper regions of the dilute solution (0.05 g/L) and weight change of the solution.

In the case of a solution with its concentration higher than 0.4 g/L, the solution became turbid homogeneously according to the evaporation of THF (Fig. 3(a)). On the other hand, low concentration solutions (lower than 0.2 g/L), the solution became turbid from the surface of the solution during the evaporation of THF. This result indicates that the particles are formed at the air/solution interface during the evaporation process of THF.

We observed the solution turbidity, as a probe of particles formation, measured by laser scattering during the evaporation of THF. Fig. 3(b) shows time courses of the weight of the solution and the scattering intensity at upper and bottom regions of the solution (0.05 g/L), respectively. The weight of the solution was decreased linearly until 20 h after mixing water. At the upper region of the solution, the scattering intensity was immediately increased for 1 h; which means that 2% of the solution evaporated after mixing. On the other hand, the scattering intensity at the bottom region was gradually increased to reach the same scattering intensity of the upper region by decreasing the solubility of polystyrene for 10 h after mixing the poor solvent. In this situation, 17% of the solution had evaporated. Since the good solvent, THF, evaporates from the surface of the solution, the polystyrene was precipitated at the air/solution interface. Thus, the upper region of the solution firstly turned turbid. As the polymers precipitated at the air/solution interface, it is suggested that the particles grew up asymmetrically as the hemispherical particles. On the other hand, in the bottom region of the solution, there was enough THF to dissolve polystyrene. The convectional flow, which was driven by the temperature and the concentration gradient due to the THF evaporation, transferred the hemispherical particles to the bottom region of the solution. The hemispherical particles were supposed to be asymmetrical shaped nuclei of polymer particles. Finally, the hemispherical shaped particles grew and dispersed in water rich medium with keeping of their unique shape.

4. Conclusions

In this report, the hemispherical particles of polystyrene were formed by adding water into dilute THF solutions of polystyrenes (lower than 0.2 g/L) and following evaporation of THF. From turbidity measurements, it suggests that the nuclei of

the hemispherical particles are formed at the air/solution interface. These hemispherical particles can be applied for optics such as a microlens arrays, electronics and biotechnology applications.

References

[1] Y. Yin, Y. Xia, Adv. Mater. 14 (2001) 605.
[2] X. Wang, C.J. Summers, Z.L. Wang, Nano Lett. 4 (2004) 423.
[3] Y. Bae, S. Fukushima, A. Harada, K. Kataoka, Angew. Chem. Int. Ed. 42 (2003) 4640.
[4] F. Caruso, Colloids and Colloid Assemblies, Wiley-VCH Verlag GmbH & Co. KGaA, Weinheim, 2004.
[5] H. Kasai, H.S. Nalwa, H. Oikawa, S. Okada, H. Matsuda, N. Minami, A. Kakuta, K. Ono, A. Mukoh, H. Nakanishi, Jpn. J. Appl. Phys. 31 (1992) L1132.
[6] PAT. JPN-2004-067883.
[7] H. Yabu, T. Higuchi, M. Shimomura, Int. J. Nanosci., in press.
[8] H. Yabu, T. Higuchi, M. Shimomura, Adv. Mater. 17 (2005) 2062.

COLLOIDS AND SURFACES
A: PHYSICOCHEMICAL AND ENGINEERING ASPECTS

Volumes 284+285 (2006)

Fabrication of photo-cross linked honeycomb-patterned films

Hiroshi Yabu [a,b], Miki Kojima [c], Mikihiko Tsubouchi [d], Shin-ya Onoue [d], Masao Sugitani [d], Masatsugu Shimomura [a,b,e,*]

[a] *Nanotechnology Research Center, Research Institute for Electronic Science, Hokkaido University, N21W10, Sapporo 001-0021, Japan*
[b] *Fronteir Research System, Institute of Physical and Chemical Science, 2-1, Hirosawa, Wako, Saitama 351-0198, Japan*
[c] *Graduate School of Science, Hokkaido University, N10W8, Sapporo 060-0810, Japan*
[d] *Kyoritsu Chemical Industry, Research Center, 5-1-2, Shiomi, Kisarazu, Chiba 292-0834, Japan*
[e] *Core Research for Evolutional Science and Technology (CREST), Japan Science and Technology Agency (JST), 4-1-8, Honcho, Kawaguchi, Saitama 332-0012, Japan*

Received 30 July 2005; received in revised form 4 October 2005; accepted 28 October 2005
Available online 9 December 2005

ELSEVIER

Amsterdam – Boston – Jena – London – New York – Oxford – Paris – Philadelphia – San Diego – St. Louis

Available online at www.sciencedirect.com
SCIENCE DIRECT
ELSEVIER
Colloids and Surfaces A: Physicochem. Eng. Aspects 284–285 (2006) 254–256
COLLOIDS AND SURFACES A
www.elsevier.com/locate/colsurfa

Fabrication of photo-cross linked honeycomb-patterned films

Hiroshi Yabu [a,b], Miki Kojima [c], Mikihiko Tsubouchi [d], Shin-ya Onoue [d], Masao Sugitani [d], Masatsugu Shimomura [a,b,e,*]

[a] *Nanotechnology Research Center, Research Institute for Electronic Science, Hokkaido University, N21W10, Sapporo 001-0021, Japan*
[b] *Fronteir Research System, Institute of Physical and Chemical Science, 2-1, Hirosawa, Wako, Saitama 351-0198, Japan*
[c] *Graduate School of Science, Hokkaido University, N10W8, Sapporo 060-0810, Japan*
[d] *Kyoritsu Chemical Industry, Research Center, 5-1-2, Shiomi, Kisarazu, Chiba 292-0834, Japan*
[e] *Core Research for Evolutional Science and Technology (CREST), Japan Science and Technology Agency (JST), 4-1-8, Honcho, Kawaguchi, Saitama 332-0012, Japan*

Received 30 July 2005; received in revised form 4 October 2005; accepted 28 October 2005
Available online 9 December 2005

Abstract

Micro-porous films are fascinating materials of potential applications for membrane filters, micro reactors and so on. Chemical and thermal stabilities of the film are significant for practical applications of these micro-porous films. Recently, the periodic micro-porous structures have been fabricated from a large variety of polymer materials by using condensed water droplet array on the polymer solution as templates. In this report, we show cross-linked honeycomb-patterned films prepared from liquid type oligomers having photo-crosslinkable groups. By controlling the UV irradiation timing, pore size of the well-arranged honeycomb-structures was regulated. After complete cross-linking by annealing, the stable film insoluble to many solvents was obtained.

Keywords: Self-organization; Photo-cross linking; Honeycomb-pattern; Micro-porous films; High stability

1. Introduction

Micro-porous films are fascinating materials of potential applications for membrane filters, micro reactors and so on [1]. There are many reports about preparation of micro-porous structures based on top-down type micro-fabrication (e.g. photo and soft lithography [2], etc.) or bottom-up type micro-fabrication (e.g. inversed opals [3], anodic alumina [4], etc.). Recently, the periodic micro-porous structures have been fabricated from a large variety of polymer materials by using condensed water droplet array on the polymer solution as templates [5–8]. Evaporation cooling on the surface of the casting solution forms water micro-droplets, and these water droplets condense and pack to cover the solution surface, then the clear solution surface turns opaque. After solvent evaporation, a honeycomb-patterned polymer film is formed.

Chemical and thermal stabilities of the film are significant for practical applications of these micro-porous films. We have reported that super-engineering plastics including polyimide [9] and sol–gel agent [10] can be used for preparation of chemically and thermally stable micro-porous films. Sirinivasarao et al. reported that poly(*p*-phenyleneethynylene) having an azide group as a side chain was cross-linked after preparation of the honeycomb structure, and the film shows high thermal stability [11]. In these cases, the honeycomb structure was firstly prepared, and then, the film was imidized or cross-linked to improve their thermal and chemical stabilities. In this report, we show cross-linked honeycomb-patterned films prepared from liquid type oligomers having photo-crosslinkable groups.

2. Experimental

Bisphenol A oligomer derivative with photo cross-linkable epoxy groups (EXA-850CRP, Dainippon Ink and Chemicals, Ink., Japan) and cationic iodide type curing agent (2074, Rhodia Japan Ltd., Japan) were purchased. Chloroform solution of photo-crosslinkable oligomer and an amphiphilic copolymer 1

* Corresponding author.
E-mail addresses: yabu@poly.es.hokudai.ac.jp (H. Yabu), shimo@poly.es.hokudai.ac.jp (M. Shimomura).

0927-7757/$ – see front matter © 2005 Elsevier B.V. All rights reserved.
doi:10.1016/j.colsurfa.2005.10.049

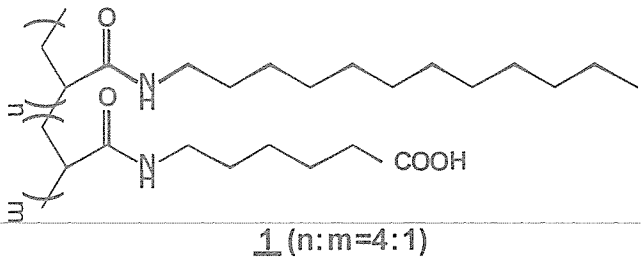

1 (n:m=4:1)

Chart 1.

(Chart 1) was prepared (solution A, oligomer: 100 mg/mL, 1: 1 mg/mL). The curing agent was dissolved in chloroform separately to prepare 10 mg/mL solution (solution B). One milliliter of solutions A and B were mixed in a glass bottle, and then, the mixed solution was casting onto a Petri dish (Ø = 3.6 cm). Humid air (relative humidity, ca. 60%) was blown at the velocity of 4 L/min onto the cast solution. During solvent evaporation, an electric balance monitored the weight change of the cast solution. Ultraviolet (UV) light (λ_{max} = 360 nm) was irradiated to the casting solution at a various stages of the solvent evaporation. Two minutes irradiation of UV light was carried at 200, 500, 700, and 1100 s of evaporation time, respectively. The surface structure of the cast film was observed by an optical microscope (BH-2, Olympus, Japan) and a scanning electron microscope (SEM, S3500N, Hitachi, Japan). The structure was finally fixed by annealing at 150 °C to complete cross-linking reaction.

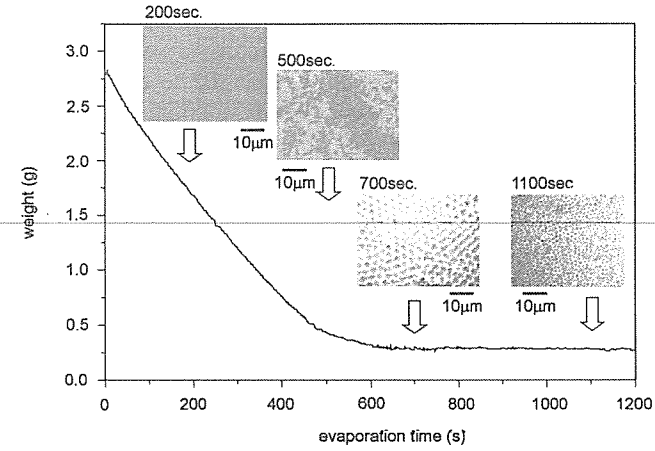

Fig. 1. A typical plot of the solvent evaporation time and weight change. Optical micrographs of UV light irradiated films at 200, 500, 700, and 1100 s after casting.

The stability of the cross-linked film against solvents was examined by immersing the prepared film in ethanol, acetone, chloroform, and pure water for 48 h. After drying the soaked films in vacuo, the surface structure was checked again by optical microscopy.

3. Results and discussion

Fig. 1 shows typical weight change of the casting solution. After ca. 500 of evaporation time, water condensation due to

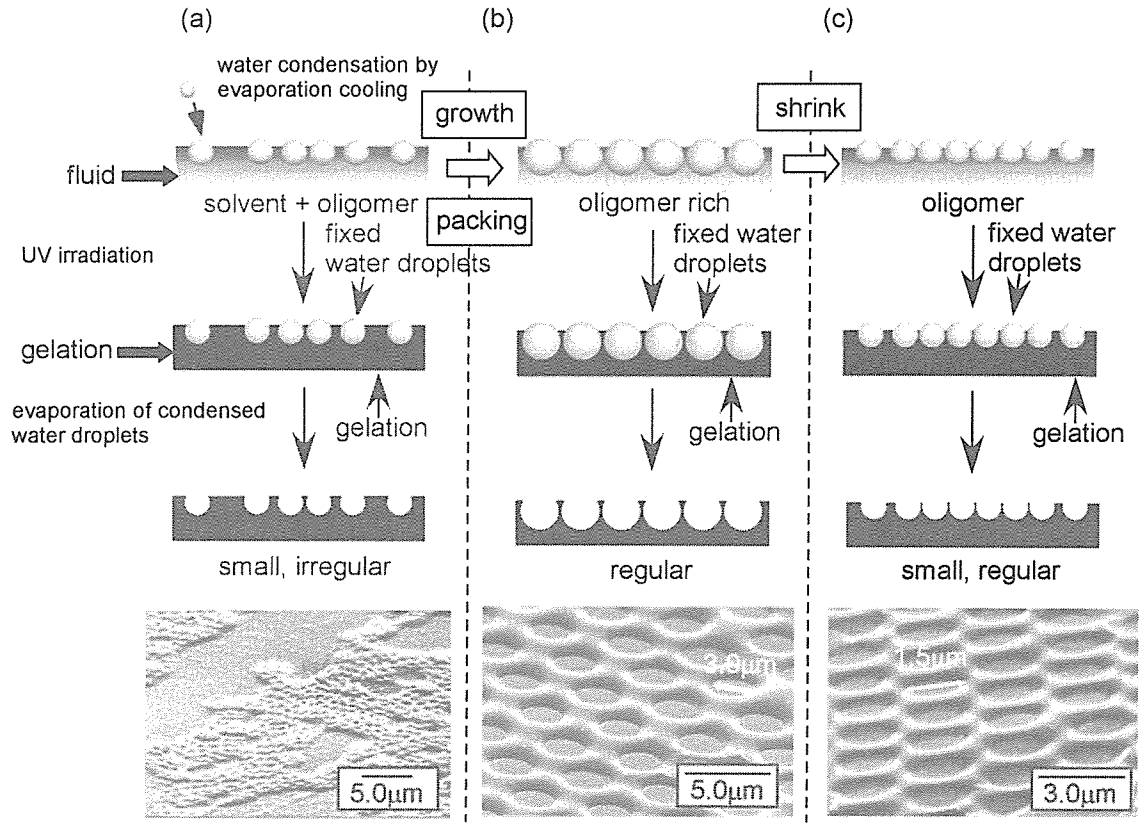

Fig. 2. Schematic illustration of structuring process of photo cross-linked micro-porous films ((a) 500 s, (b) 700 s, and (c) 1100 s after casting). A scanning electron micrograph of each stage is also shown at the bottom of each column. All samples were tilted 70°.

the evaporation cooling of the solution surface was observed by in situ optical microscopy. The temperature of solution surface became ca. 10 °C, which was lower than the dew point (in our experimental condition, the dew point was 15–20 °C). The condensed water droplets grew up, and they were packed during evaporation of solvent. The surface cooling and increased viscosity of the solution as well as surface covering by condensed water droplets reduced the solvent evaporation rate. The solvent completely evaporated ca. 650 s after casting.

Inset images of Fig. 1 shows optical micrographs after UV irradiation at the various stages of evaporation. When UV light was irradiated at 200 s of evaporation time, the solution gelated soon after the irradiation. Optical microscopy shows a smooth surface of the gelled film. The water droplets start to condense 400 s after casting. Movement of water droplets was freezing due to the surface gelation induced by photo-cross linking. Therefore, small sized pores (ca. 1 μm) were remained unchanged during further evaporation after UV irradiation at 500 s after casting. The condensed water droplets did not grow up because of the gelation of the solution surface. Moreover, the pores were irregularly arranged because of the freezing of lateral movement of the condensed water droplets. Fig. 2(a) shows the schematic illustration of the structuring process and SEM image of the film cross-linked at 500 s of evaporation time. Small pores were aggregated and the aggregates distributed like "islands" on the cross-lined film. After 600 s passed, the water droplets covered the whole region of the solution surface, and 700 s of evaporation time, regular hexagonal arrangement of water droplets was formed. After irradiation of UV light, hexagonally packed 3 μm micropore array was observed. In this case, the water droplets grew up and laterally moved to well-ordered packing by capillary force (Fig. 2(b)). The SEM image of the cross-linked film clearly shows a well-ordered honeycomb liked structure. The condensed water droplet size decreased after 800 s from solution cast. On this stage, the size of the water droplets decreased with time. When the UV light irradiated at 1100 s after casting, the pore size of the honeycomb structure was reduced to 1.5 μm. The surface temperature of the liquid oligomer rose up to the room temperature, which was higher than the dew point, because there was no evaporation cooling any more. As a result, the template water droplets shrunk (Fig. 2(c)). In the case of 1500 s after casting, the water droplets were completely evaporated and a flat film was obtained after UV exposure. These results indicate that well-arranged honeycomb-like porous film can be obtained after evaporation of solvent with controlling its pore size.

After complete cross-linking by thermal annealing at 150 °C, we checked the chemical stability of the prepared film by immersing into several solvents. After immersing in chloroform, acetone, ethanol, and water for 48 h, the honeycomb structure was kept even though immersing in chloroform, which is a good solvent of cross-linkable oligomer.

4. Conclusion

We show the simple preparation method of honeycomb-patterned micro-porous films from liquid type photo-cross linking oligomer by using condensed water droplets on the solution surface as templates. By controlling the UV irradiation timing, pore size of the well-arranged honeycomb-structures was regulated. After cross-linking completed by annealing, the stable film insoluble to many solvents was obtained. The highly stable well-arranged micro-porous films can be easily prepared on the wide surface area by using the coating apparatus described before [12] with UV irradiation. These stable honeycomb-patterned micro-porous films can be applied for micro reactors, stable membrane filters, and other applications in the fields of photonics, electronics and biotechnologies.

Acknowledgement

This work was partly supported by grant-in-aid for Scientific Research, MEXT, Japan.

References

[1] J.E. Barton, D.W. Odem, Nano. Lett. 4 (8) (2004) 1525.
[2] Y. Xia, G.M. Whitesides, Angew. Chem. Int. Ed. 37 (1998) 550.
[3] T. Cassagneau, F. Caruso, Adv. Mater. 14 (1) (2002) 34.
[4] H. Masuda, H. Asoh, M. Watanabe, K. Nishio, M. Nakao, T. Tamamura, Adv. Mater. 13 (3) (2001) 189.
[5] G. Widawski, M. Rawiso, B. François, Nature 369 (1994) 387.
[6] O. Karthaus, N. Maruyama, X. Cieren, M. Shimomura, T. Hasegawa, T. Hashimoto, Langmuir 16 (19) (2000) 6071.
[7] M. Stenzel, Aust. J. Chem. 55 (2002) 239.
[8] (a) H. Yabu, M. Shimomura, Langmuir 21 (5) (2005) 1709;
(b) H. Yabu, M. Takebayashi, M. Tanaka, M. Shimomura, Langmuir 21 (8) (2005) 3235;
(c) H. Yabu, M. Shimomura, Chem. Mater. 17 (21) (2005) 5231.
[9] H. Yabu, M. Tanaka, K. Ijiro, M. Shimomura, Langmuir 19 (15) (2003) 6297.
[10] (a) O. Karthaus, X. Cieren, N. Maruyama, M. Shimomura, Mater. Sci. Eng. C 10 (1–2) (1999) 106;
(b) H. Yabu, M. Shimomura, Int. J. Nanosci. 1 (5–6) (2002) 673.
[11] B. Erdogan, L. Song, J.N. Wilson, J.O. Park, M. Srinivasarao, U.H.F. Bunz, J. Am. Chem. Soc. 126 (12) (2004) 3678.
[12] H. Yabu, M. Shimomura, Adv. Func. Mater. 15 (4) (2005) 575.

COLLOIDS AND SURFACES
A: PHYSICOCHEMICAL AND ENGINEERING ASPECTS

Volumes 284+285 (2006)

Multiple-periodic structures of self-organized honeycomb-patterned films and polymer nanoparticles hybrids

Hiroshi Yabu [a,b], Kouta Inoue [c], Masatsugu Shimomura [a,b,d,*]

[a] *Nanotechnology Research Center, Research Institute for Electronic Science, Hokkaido University, N21W10, Sapporo 001-0021, Japan*
[b] *Frontier Research System, Institute of Physical and Chemical Research (RIKEN Institute), 2-1, Hirosawa, Wako, Saitama 351-0198, Japan*
[c] *Faculty of Science, Hokkaido University, N10W8, Sapporo 060-0810, Japan*
[d] *Core Research for Evolutional Science and Technology (CREST), Japan Science and Technology agency (JST), 4-1-8, Honcho, Kawaguchi, Saitama 332-0012, Japan*

Received 23 June 2005; received in revised form 4 October 2005; accepted 28 October 2005
Available online 4 January 2006

ELSEVIER

Amsterdam – Boston – Jena – London – New York – Oxford – Paris – Philadelphia – San Diego – St. Louis

Available online at www.sciencedirect.com
SCIENCE DIRECT
ELSEVIER
Colloids and Surfaces A: Physicochem. Eng. Aspects 284–285 (2006) 301–304
COLLOIDS AND SURFACES A
www.elsevier.com/locate/colsurfa

Multiple-periodic structures of self-organized honeycomb-patterned films and polymer nanoparticles hybrids

Hiroshi Yabu [a,b], Kouta Inoue [c], Masatsugu Shimomura [a,b,d,*]

[a] *Nanotechnology Research Center, Research Institute for Electronic Science, Hokkaido University, N21W10, Sapporo 001-0021, Japan*
[b] *Frontier Research System, Institute of Physical and Chemical Research (RIKEN Institute), 2-1, Hirosawa, Wako, Saitama 351-0198, Japan*
[c] *Faculty of Science, Hokkaido University, N10W8, Sapporo 060-0810, Japan*
[d] *Core Research for Evolutional Science and Technology (CREST), Japan Science and Technology agency (JST), 4-1-8, Honcho, Kawaguchi, Saitama 332-0012, Japan*

Received 23 June 2005; received in revised form 4 October 2005; accepted 28 October 2005
Available online 4 January 2006

Abstract

We show the preparation of honeycomb-nanoparticles hybrid structures by simple casting of nanoparticle dispersion onto the self-organized honeycomb-patterned films. The polystyrene honeycomb-patterned films were prepared by the "Breath Figure" method. The hydrophobic polystyrene honeycomb-patterned films were treated by UV-O_3 to improve the wettablity. A newly developed sliding apparatus were used for embedding the submicron polystyrene particles. Finally, we obtained the multiple-periodic structure of the honeycomb-patterned film and nanoparticles.

Keywords: Honeycomb-patterned films; Polymer nanoparticles; Multi-periodicity; Self-organization; Polymer films

1. Introduction

This paper describes the fabrication of hybrid structures of honeycomb-patterned micro-porous films and polymer nanoparticles. The periodic structure in the range of submicron or micron scale has received great interest for potential applications in the fields of photonics [1], electronic [2] and biotechnologies [3]. In the photonics field, the periodic microstructures can be utilized for photonic crystals [4]. There are many reports about the fabrication of photonic crystals produced by using conventional photolithography [5], two-photon laser nanofabrication [6], self-assembly of colloidal particles [7] (colloidal crystals), inversed opals [8] and so on.

Microstructures with multiple periodicities can be applied for photonic crystals, which have two or more stop bands. The conventional lithographic technologies can fabricate such microstructures with multiple periodicities. However, it requires elaborate multiple processes and expensive instruments. And these lithographic methods applied to limited materials (e.g. silicon based semiconductors, metals, and so on). It was reported that "template-directed self-assembly" process, which embeds polymer nanoparticles onto patterned silicon substrate, enabled to easily produce such multiple periodic structures [9]. However, fabrication of multiple-periodic microstructure of hydrophobic polymeric materials is difficult to prepare by using the self-assembly system because the particle dispersion (usually water dispersion) dewetted on the hydrophobic polymer microstructures.

Recently, periodic micro-porous structures were fabricated from variety of polymer materials by using condensed water droplets on the polymer solution as templates ("Breath Figure" method) [10–13]. Hexagonally packed water micro-droplets are formed by evaporative cooling on the surface of the casting solution, and these water droplets are transferred to the solution front by convectional flow or capillary force. When the water droplets condense on the solution surface, the clear solution turns opaque. After solvent evaporation, a honeycomb-patterned polymer film is formed with the water droplet array acting as a template; the water droplets themselves evaporate soon after the solvent. These micro-porous films can be applied for pho-

* Corresponding author. Fax: +81 48 462 4630.
E-mail address: shimo@poly.es.hokudai.ac.jp (M. Shimomura).

0927-7757/$ – see front matter © 2005 Elsevier B.V. All rights reserved.
doi:10.1016/j.colsurfa.2005.10.082

tonic crystals since they have highly ordered periodic change of reflective indices. Actually, we reported that these micro-porous structure shows stop band in the infrared wavelength region [14].

Here, we show the fabrication of periodic micro-structured films having multiple periodicities by hybridization of the honeycomb-patterned films and polymer nanoparticles. Micron scale honeycomb-patterned films were prepared from polystyrene and amphiphilic copolymer [11(b)]. To embed polymer nanoparticles in the honeycomb pores, a dispersion of polystyrene was cast onto the honeycomb-patterned films. However, the polystyrene honeycomb-patterned films are hydrophobic surface, thus, water dispersion of particles were not wet on them. To improve the surface wettability, UV-ozone (O_3) treatment was performed. And the submicron sized polystyrene particles embedded only in the honeycomb pores by casting the particle dispersion on the hydrophilic honeycomb-patterned films. Using a newly developed instrument, which coats the particle dispersion continuously onto the substrate surface, performed the dispersion casting process. The formation process and size variation of the honeycomb-particles hybrid structures are discussed.

2. Experimental details

2.1. Preparation of honeycomb-patterned films

Polystyrene (PSt, $M_w = 280{,}000$) was obtained from Aldrich, USA. The amphiphilic copolymer **1** was synthesized according to the literature [10(c)]. PSt and **1** (weight ratio: 10:1) were dissolved in chloroform at a concentration of 5 mg/mL. Five milliliter of homogeneous solution was cast onto a Petri dish (diameter = 9 cm) at room temperature, under humid air (relative humidity, 80%) applied by an air pump (current velocity, 2 L/min). The honeycomb structure was observed by optical microscopy (BH-2, Olympus, Japan) and scanning electron microscopy (S-3500N, Hitachi, Japan).

2.2. UV-O_3 treatment of the polystyrene honeycomb-patterned films

An ultraviolet and ozone exposure (OC-250615-D + A, IWASAKI DENKI, Co. Ltd., Japan) was used to expose the UV-O_3. As-prepared honeycomb-patterned films were set under in the chamber of UV-O_3 exposure, and they were treated by UV-O_3 for 10–60 min at normal pressure. Ten milliliters of membrane-filtered water (millipore filter) were dropped onto the UV-O_3 treated honeycomb-patterned films, and then, the water contact angles were measured by using a contact angle analyzer (Z-1, Erma, Germany). The elemental analysis of the surface was performed by X-ray photoelectron spectroscopy (XPS, JPS-9200, JEOL, Japan). X-ray souse, X-ray energy and pass energy were Al Kα, 1486.6, and 10 eV, respectively.

2.3. Embedding the PSt particles in the honeycomb pores

Water dispersions of PSt colloidal particles (diameters; 500 nm, 750 nm, and 2.5 μm) were obtained from Duke scientific co. Ltd., USA. The hydrophilic honeycomb-patterned films were cut by a surgical knife as a 10 mm × 10 mm and fixed on a glass plate (76 mm × 26 mm, Matsunami, Japan). The glass plate was fixed on the substrate holder. Another bare glass plate was fixed on the clump, which can be straightly moved by a computer controlled driving system (Fig. 1c) [15]. These two glass plates were overlapped 30 mm in parallel with 2 mm spacing. Fifty microliter of the colloidal suspension was filled in the spacing between two glass plates. One glass slide was moved straightly at the velocity of 10 μm/s.

3. Results and discussion

3.1. Honeycomb-patterned films

Highly ordered honeycomb-patterned films with 5 μm pores were formed. SEM image clearly shows hexagonally arranged micro-pores (Fig. 2a). The inset of Fig. 2a shows the cross-section of honeycomb-patterned film. The film is consisted of two layers (upper and bottom) supported by pillars on each vertex of hexagon [16]. Therefore, all pores are connected each other.

3.2. Surface hydrophilization

To embed polymer nanoparticles in the honeycomb pores, a dispersion of polystyrene was cast onto the honeycomb-patterned films. We have reported the honeycomb-patterned film shows superhydrophobicity based on the Lotus leaf effect [17].

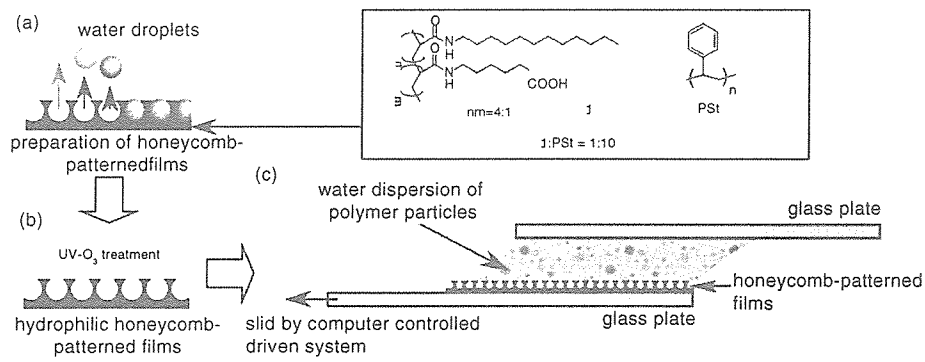

Fig. 1. Schematic illustration of preparation of: a honeycomb-patterned film (a); UV-O_3 treatment (b); and nanoparticles embedding process (c).

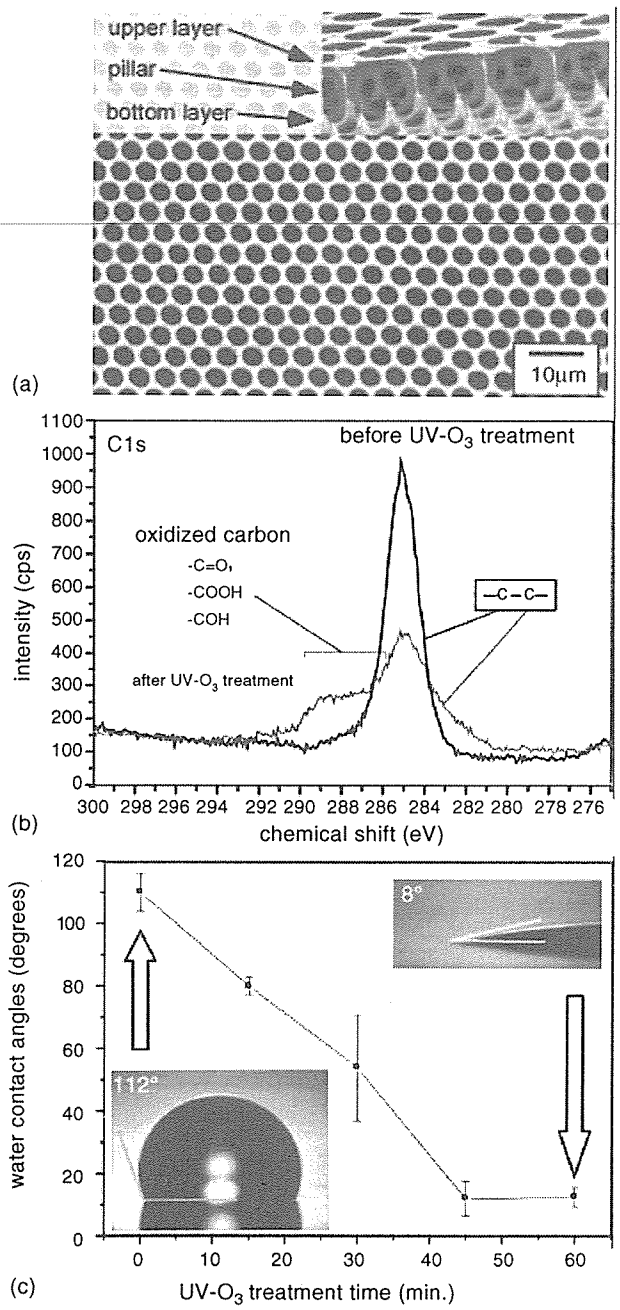

Fig. 2. (a) Scanning electron micrograph of the honeycomb-patterned film from PSt and 1. (b) XPS spectra of the honeycomb-patterned film before and after exposure of UV-O_3. (c) UV-O_3 Exposure time dependence on the water contact angles on the honeycomb-patterned films.

Thus, the honeycomb-patterned film repels the water dispersion of polystyrene particles. To introduce the polystyrene particles into the pores by using the capillary force, the wettability of the surface should be improved.

We use the UV-O_3 treatment to convert the surface properties of the honeycomb-patterned films. Ozone molecules generated from oxygen by UV irradiation ($\lambda = 185$ nm), photo chemically oxidizes hydrocarbons on the film surface under UV irradiation ($\lambda = 254$ nm).

To reveal the chemical composition of the surface, the elemental analysis of the UV-O_3 treated honeycomb-patterned film was performed by the XPS measurement. Fig. 2b shows the XPS spectrum obtained from the honeycomb-patterned films of PSt before (black line) and after (gray line) the UV-O_3 treatment. A single sharp peak attributed to carbon 1s (C1s) of polystyrene around 285 eV was obtained. After the UV-O_3 treatment, the peak of C1s is consisted of two components. One is a sharp peak on 285 eV, the other is a broad peak around up to 290 eV. These peaks indicate the carbon groups and formation of hydrophilic –C=O, –COOH, and –COH groups on the surface of honeycomb-patterned films, respectively.

The hydrophilicity of the honeycomb-patterned films was evaluated by water contact angle measurement. The contact

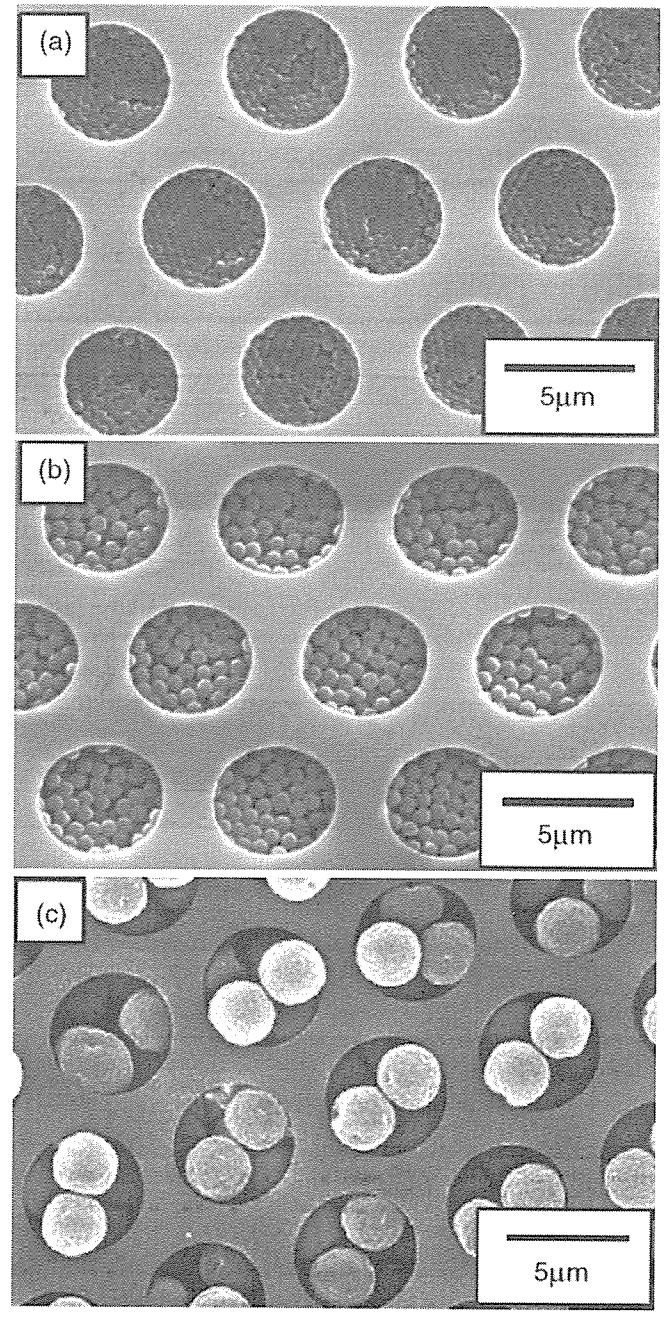

Fig. 3. Scanning electron micrographs of nanoparticles embedded honeycomb-patterned films (particle size = 500 nm (a), 750 nm (b), 2.1 μm).

angles of water on the honeycomb-patterned film decreased when the treatment time increased (Fig. 2c). After 45 min irradiation, the water contact angle became the minimum value, ca. 10°. The newly formed functional groups change the surface properties of the honeycomb-patterned films from hydrophobic to hydrophilic.

3.3. Embedding the polystyrene nanoparticles in the honeycomb pores

After UV-O_3 treatment, the water dispersion of polymer particles wets on the honeycomb-patterned films. The water dispersion was injected in the gap between the hydrophilic honeycomb-patterned film and the upper glass plate. After slowly sliding of the honeycomb-patterned film, thin liquid film of the particle dispersion was formed. The polymer particles were embedded on the pores of honeycomb-patterned film after evaporation of water by capillary force [18].

After embedding the polystyrene particles in the honeycomb pores, the hybrid structure was observed by SEM. Fig. 3a shows a 5 μm-pore honeycomb-patterned film with packed 500 nm polystyrene particles in its pores. The particles were well packed by capillary force during evaporation of water, and there are few particles on the rim of honeycomb structures because the particles were drug into pores by strong capillary force. In the case of changing the diameter of particles, the number of particles embedded in the pores can be controlled (Fig. 3b and c). These results indicate that the particles were embedded in the honeycomb pores independent from the particle size/pore size ratio. These results also indicates the honeycomb-nanoparticles hybrid structure can be prepared by simple UV-O_3 treatment and casting the particle suspension.

The each film shows stronger light scattering from the surface than the only honeycomb-structured film. Especially, in the case of using 500 nm particles, the film shows specific color when it was sputtered with Pt/Pd. This means the prepared film can be applied for optical film including light diffuser, reflector, grating and so on.

4. Conclusions

We show the preparation of honeycomb-nanoparticles hybrid structures by simple casting of nanoparticles dispersion onto the self-organized honeycomb-patterned films. A newly developed sliding apparatus were used for embedding the submicron polystyrene particles. The hydrophobic polystyrene honeycomb-patterned films were treated by UV-O_3 to improve the wettability. We have found a preparation method of nanoparticles from functional polymers [19]. The hybrid structure of honeycomb and nanoparticles can be utilized not only for photonic band gap materials but also for optical memories, microelectrodes and other practical applications by changing the embedded particles such as micro spheres, dyes, and metal nanoparticles.

Acknowledgement

This research was partly supported by Grant-in-Aid for Scientific Research, MEXT, JAPAN, No.14205132, No.14000563. We would like to thank Mr. Osamu Haruta for helping XPS measurements.

References

[1] S. Noda, A. Chutinan, M. Imada, Nature 407 (2000) 608.
[2] N. Fukuda, M. Shimomura, Int. J. Nanosci. 1 (5–6) (2002) 551.
[3] T. Nishikawa, M. Nonomura, K. Arai, J. Hayashi, T. Sawadaishi, Y. Nishiura, M. Hara, M. Shimomura, Langmuir 19 (15) (2003) 6193.
[4] J.D. Joannopoulos, R.D. Meade, J.N. Winn, Photonic Crystals—Molding the Flow of Light, Princeton University Press, New Jersey, 1995.
[5] Y. Akahane, T. Asano, B.-S. Song, S. Noda, Appl. Phys. Lett. 83 (8) (2003) 1512.
[6] K. Kaneko, H.-B. Sun, X.-M. Duan, S. Kawata, Appl. Phys. Lett. 83 (11) (2003) 2091.
[7] H. Miguez, S.-M. Yang, G.A. Ozin, Langmuir 19 (8) (2003) 3479.
[8] T. Casssagneau, F. Caruso, Adv. Mater. 14 (22) (2002) 1629.
[9] (a) Y. Xia, Y. Yin, Y. Lu, J. Mclellan, Adv. Funct. Mater. 13 (2003) 907;
(b) Y. Yin, Y. Lu, B. Gates, Y. Xia, J. Am. Chem. Soc. 123 (2001) 8718.
[10] (a) G. Widawski, M. Rawiso, B. François, Nature 369 (1994) 387;
(b) B. François, O. Pitois, J. François, Adv. Mater. 7 (1995) 1041.
[11] (a) O. Karthaus, N. Maruyama, X. Cieren, M. Shimomura, T. Hasegawa, T. Hashimoto, Langmuir 16 (19) (2000) 6071;
(b) H. Yabu, M. Shimomura, Langmuir 21 (4) (2005) 1709;
(c) T. Nishikawa, R. Ookura, J. Nishida, K. Arai, J. Hayashi, N. Kurono, T. Sawadaishi, M. Hara, M. Shimomura, Langmuir 18 (15) (2002) 5734.
[12] M. Stenzel, Aust. J. Chem. 55 (2002) 239.
[13] M. Srinivasarao, D. Collings, A. Philips, S. Patel, Science 292 (2001) 79.
[14] N. Kurono, R. Shimada, T. Ishihara, M. Shimomura, Mol. Cryst. Liq. Cryst. 277 (2002) 285.
[15] H. Yabu, M. Shimomura, Adv. Funct. Mater. 15 (4) (2005) 575.
[16] (a) H. Yabu, M. Tanaka, K. Ijiro, M. Shimomura, Langmuir 19 (15) (2003) 6297;
(b) T. Yonezawa, S. Onoue, N. Kimizuka, Adv. Mater. 13 (2001) 140;
(c) C.S. Lee, N. Kimizuka, PNAS 99 (2002) 4922.
[17] (a) H. Yabu, M. Takebayashi, M. Tanaka, M. Shimomura, Langmuir 21 (8) (2005) 3235;
(b) H. Yabu, M. Shimomura, Chem. Mater. 17 (21) 5235.
[18] N.D. Denkov, O.D. Velev, P.A. Kralchevsky, I.B. Ivanov, H. Yoshimura, K. Nagayama, Nature 361 (1993) 26.
[19] H. Yabu, T. Higuchi, M. Shimomura, Adv. Mater. 17 (17) (2005) 2062.

Available online at www.sciencedirect.com
SCIENCE DIRECT®
Colloids and Surfaces A: Physicochem. Eng. Aspects 284–285 (2006) 315–319
COLLOIDS AND SURFACES A
www.elsevier.com/locate/colsurfa

Light-propagation patterns in freestanding two-dimensional colloidal crystals

Sachiko Matsushita [a,c], Masatsugu Shimomura [a,b,*]

[a] *Dissipative-Hierarchical Structures Lab., Spatio-Temporal Functional Group, RIKEN Frontier Research System, 2-1 Hirosawa, Wako, Saitama 351-0198, Japan*
[b] *Nanotechnology Research Center, Research Institute for Electronic Science, Hokkaido University, N21 W10, Kita-Ku, Sapporo 060, Japan*
[c] *Department of Integrated Sciences in Physics and Biology, Colloge of Humanities and Sciences, Nihon University, Japan*

Received 9 June 2005; received in revised form 30 December 2005; accepted 4 January 2006
Available online 21 February 2006

Abstract

This paper reports the preparation of freestanding two-dimensional (2D) particle arrays, which fine particles are packed in highly dense and oriented manner. To fabricate freestanding 2D arrays, sintering process of the polymer particles (3.06, 1.034, and 0.491 μm diameter) was examined. The sintered 2D particle arrays on glass substrates were easily peeled off as a freestanding film by soaking into water. The freestanding 2D particle arrays were stable enough in room temperature. They show the iridescent colors due to their optical periodicity. To convince the layer number of those freestanding 2D particle arrays, fluorescent polystyrene particles were added in the arrays. Fluorescent light propagation patterns in the arrays suggest that the freestanding films were monolayers. The transmission spectra of the freestanding film were also examined.

Keywords: Self-assembly; Photonic crystal; Evanescent field; Self-organized; Particle

1. Introduction

Two-dimensional (2D) particle arrays, which fine particles of polystyrene (PSt) [1–3], silica [4–6], or proteins [7,8] are two-dimensionally packed in highly dense and oriented manner [1], have been attracted as high-density optical memory device [9,10], photocatalytic systems [5,6], and quasi-2D photonic-crystal [11–13] because of their attractive features such as large domains, controllability of the layer number, easy and fast producibility (one sheet of 25 mm × 30 mm wide is prepared less than 30 min), et al.

Two-dimensional particle arrays are prepared on flat surfaces by the self-assembled process of particle suspension. The driving force of particle accumulation is the capillary force at the meniscus of a solution–substrate interface [14]. Therefore, the influence of substrates has been the intrinsic character of 2D array. If we could prepare 2D arrays without substrates, in other words "freestanding 2D arrays", they would have new aspects: for example, a recent theoretical calculation on photonic crystals predicts that freestanding 2D particle arrays might have sharper transmission-spectra than the spectra of 2D particle arrays on substrates [15].

Matsushita et al. have fabricated freestanding 2D particle arrays by using the photo-cross-linking technique. A photoactive cross-linker was connected to the particles [16]. However, photoactive cross-linker was piled up on arrays, then the original quality (light propagation inside of the particles, for example [17,18]) of 2D particle arrays became worse after photo-cross-linking. Other conceivable method to fabricate freestanding 2D particle arrays is a sintering technique. The sintering technique has attractive features, because sintering processes of inorganic and organic materials [19] are well known both theoretically [20] and experimentally [21]. In this paper, we report the preparation of freestanding monolayers of 2D PSt-particle arrays by the sintering technique. To show the freestanding films maintain the original quality of 2D particles, the fluorescence microscopic observation of light propagation patterns in the arrays and the transmission spectra measurement were employed.

2. Materials and methods

2.1. Array preparation

A schematic fabrication process of the freestanding 2D particle arrays is shown in Fig. 1. The 2D particle arrays were prepared from the water suspensions of commercial monodis-

* Corresponding author. Tel.: +81 11 706 9368; fax: +81 11 706 9363.
E-mail address: sachiko_matsushita@riken.jp (M. Shimomura).

0927-7757/$ – see front matter © 2006 Elsevier B.V. All rights reserved.
doi:10.1016/j.colsurfa.2006.01.028

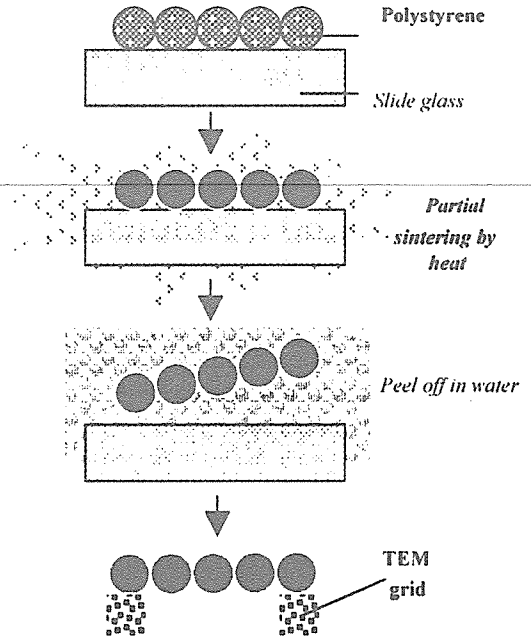

Fig. 1. Schematic procedures for the fabrication of freestanding two-dimensional particle arrays by sintering.

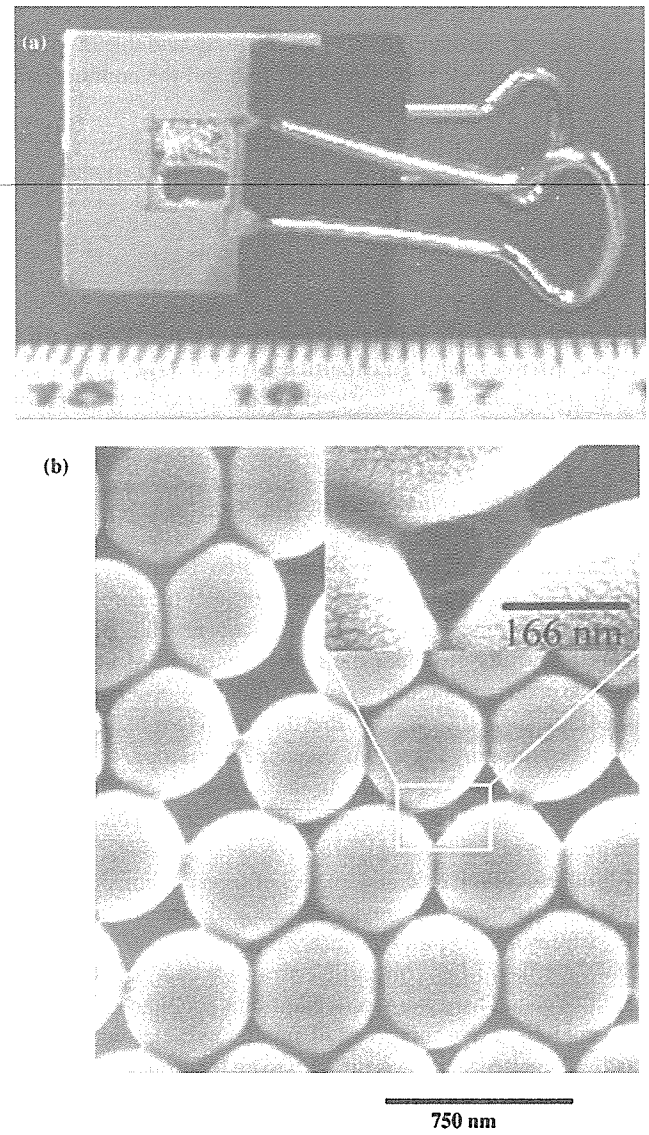

Fig. 2. The digital camera image (a) of a freestanding monolayer of 1 μm diameter polystyrene particles, and the scanning electron microscopic images (b) of the polystyrene particle's (0.491 μm diameter) array after sintering.

persed PSt microparticles (3.06 ± 0.08 μm, 1.034 ± 0.020 μm, 0.491 ± 0.004 μm Nanosphere™ Size Standards, NIST Traceable Polystyrene Polymer, Polysciences, Inc.). The self-assembly technique for the preparation of 2D particle arrays was originally proposed by Nagayama et al. [22]. Due to water evaporation and capillary forces, the particles suspended in water formed 2D arrays on a nonfluorescent glass substrate (Matsunami Co., Japan). The speed of array formation was controlled at rates from 1.0 to 3.0 μm/s by moving the substrate horizontally. The particle assembly process was observed by using a CCD camera. Well-ordered 2D arrays with the typical dimensions of 25 mm × 30 mm were prepared. The details of the fabrication process was mentioned elsewhere [23].

We prepared composite arrays from two types of fluorescent particles, i.e., red ($\lambda_{ex}/\lambda_{em}$ 541/612 nm; Polymer Microspheres, Red Fluoresceing, Duke Scientific Corp.) and green ($\lambda_{ex}/\lambda_{em}$ 458/540 nm; fluoresbrite carboxylate microspheres, Polysciences Inc.) with nonfluorescent particles (Particle-Size Standards, NIST Traceable, Duke Scientific Corp.) such that the fluorescent particles were present at a relatively low fraction, i.e., 1:1:1000 (red-green-nonfluorescent).

2.2. Freestanding monolayers preparation

Well-ordered 2D particle arrays thus formed were put into an electric oven and heated at 80 °C for 30 min. Fig. 2b shows the scanning electron microscopic (SEM) image (S-900, Hitachi) of the sintered 0.491 μm particle's array. The formation of interparticle contacts and neck growth was observed (Fig. 2b, inset). The diffraction patterns of He–Ne laser verified the hexagonal closest particle packing after the sintering.

2.3. Microscopic observations

The sintered particle arrays were soaked into pure water. They were peeled off softly from the substrate by a teflon tweezers. As holders, a handmade paper grid with a 5 mm square hall for the digital camera image, a cupper grid with 25 μm square halls (MICRON GRIDE mesh, NISSHIN EM Co., Ltd.) for the optical microscopic observations, and a SUS mesh with 50 μm square halls (SUS-316, TAIYO WIRE CLOTH Co., Ltd.) for the transmission spectra measurement (UV3100, Shimadzu Co.) were used.

2.4. Transmission spectra measurement

The transmission spectra measurement was also carried out at normal incidence. The measurement area was 1 mm × 5 mm.

Our UV–VIS-NIR spectroscopy is a double beam system. The references of freestanding 2D particle array and the 2D particle array on a substrate were the SUS mesh and the nonfluorescent glass substrate, respectively.

3. Results and discussions

3.1. Digital camera image

The arrays were peeled softly and moved from the glass substrate to the holder using Teflon tweezers in water. The maximum size of the freestanding 2D particle array is larger than 8 mm^2. Their iridescent colors clearly show the periodicity of particle packing (Fig. 2a).

3.2. Fluorescent optical microscopy images

The tilted-SEM and/or atomic force microscopy (AFM) observation are/is also useful method(s) to measure the number of the layers. However, the thin and flexible freestanding monolayer rolls up under the high-vacuum SEM observation. The warped freestanding array is difficult to observe by AFM, especially to get the evidence that the array is a monolayer. Thus, the authors employed the fluorescence microscopic observations of light propagation patterns in the arrays. One of the authors had reported that the light propagation patterns in the arrays tell the number of the layers [17,18].

Fluorescent microscopic images of freestanding 3.06, 1.034, and 0.491 μm particle arrays on TEM grids are shown in Fig. 3. Those freestanding monolayers are mechanically fragile. Fig. 3b shows a broken 1.034 μm particle array was caught at the edge of the TEM grid. There were some additional problems. The thinner freestanding arrays composed of smaller particles warped more easily. The warped array is difficult to be focused on a wide area, even the size of a TEM grid's hole (25 μm × 25 μm) (Fig. 3c). However, as discussed below, these problems did not inhibit their correct observations to know the number of the layers from their light propagation patterns.

3.3. Light propagation in the nonfluorescent particles

In the case of the monolayer of a 2D array on a substrate, we can observe six-fold symmetrical light-propagation pattern. The emitted light from fluorescent PSt particles propagated along the rows of adjoining nonfluorescent hexagonally-closest-packed spheres, because PSt has the higher refractive index than air. The beautiful crescent shapes of scattered light between the substrate and the particles can be observed between adjoining nonfluorescent particles (Fig. 4a) [17]. On the other hands, in these freestanding array's images, those light-propagation patterns were less observed (Fig. 4b). One of the reasons is the absence of substrate, i.e., there is no reflected light from a substrate to the objective lens. The dot-type light emission at a domain edge (four orange bright dots in Fig. 3b) is the alternative evidence of the light propagation in the adjoining nonfluorescent particles.

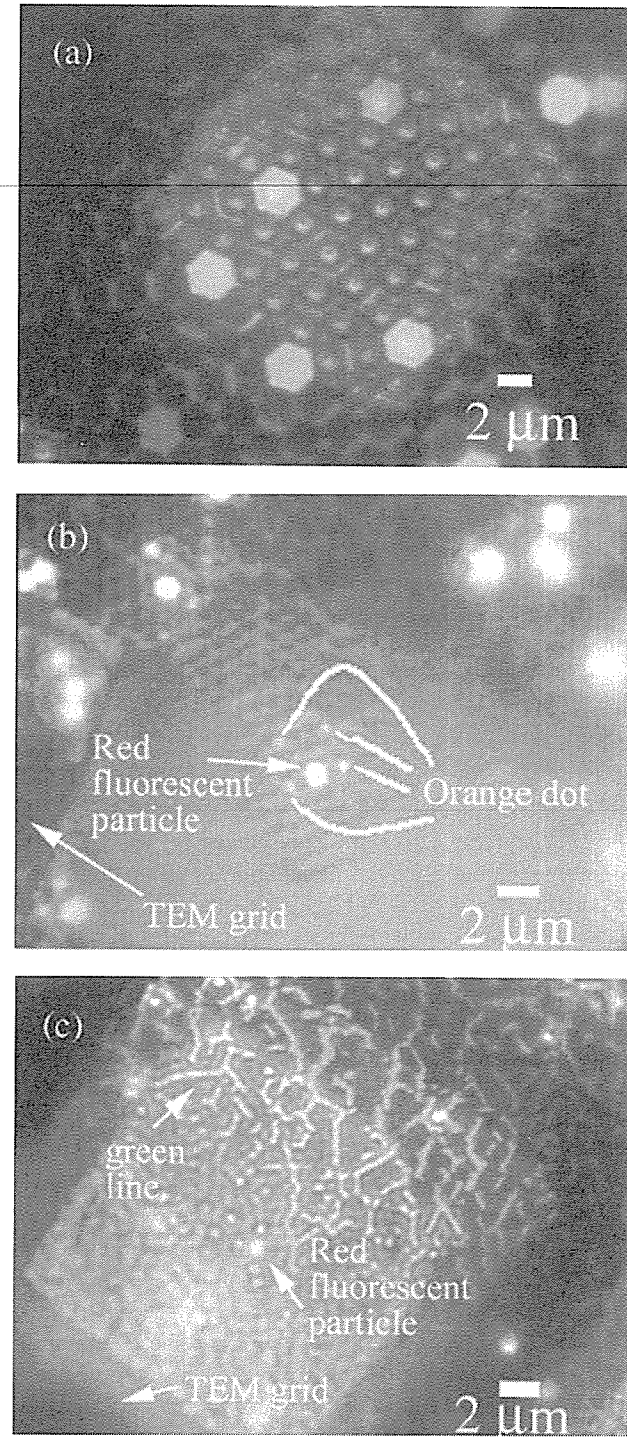

Fig. 3. The fluorescent micrographs of the two-dimensional arrays of (a) 3.06, (b) 1.034, and (c) 0.491 μm diameter polystyrene particles. Those arrays included red and green fluorescent particles. The black square area is the cupper TEM grid.

This light propagation in the nonfluorescent particles is a key to know the number of the layers. When the array is a bilayer, we can observe a small triangle pattern composed of three bright dots from the top view; when the array is a triple layer, we can observe a flower-like patterns composed of seven bright dots in

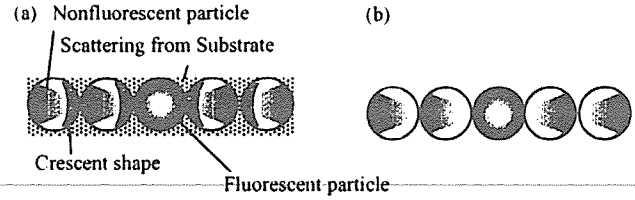

Fig. 4. The schematic diagrams of the top view of light propagation in monolayers of monodisperse polystyrene particles consisting of the mixture of fluorescing particles with (a) and without (b) a substrate.

hexagonal closest packing, and a big triangle pattern compose of six bright dots in face-centered cubic packing [17]. Because we cannot observe those multi-layers' patterns in Fig. 3a and b, we may say that those 3.06 and 1.034 μm particle arrays are monolayers.

3.4. Polymer diffusion

We show the visual evidence of the polymer diffusion process during the sintering. With regard to 0.491 μm diameter particles arrays, green fluorescent particles cannot observe, but green fluorescence lines at the edge of the domains. On the other hand, the red fluorescent particles maintain their particle forms (Fig. 3c). Here, we would like to explain the sintering process in detail.

We employed the polymer-diffused sintering process to fabricate freestanding particle monolayers. Surface polymer of the particles transport and form a film-like morphology for minimizing the total surface energy at the sintering temperature [24]. The synthetic method of the dye incorporation into polymer particles differs with the type of the dye. That is, the incorporated area of the fluorescent dyes is different between the green and red particles.

Our green fluorescence dye exists on the outside 10% radii of the particles. It is easily diffused with the surface polymer (http://www.polysciences.com). Consequently, the small particles (0.491 μm) could not be observed as green full-circle patterns after the sintering. Meanwhile, our red fluorescence dye exists in the whole part of the particle (http://www.dukescientific.com). Thus, the red small particles could be observed even after the sintering and show the evidence that this layer is monolayer.

3.5. Transmission spectra of the freestanding array

The transmission spectra of the freestanding 2D particle array and the 2D particle array on a substrate are shown in Fig. 5. This spectrum of the 2D particle array on a substrate was obtained after five repetitions of polynomial smoothing.

Strong extinction peaks were observed in both samples, indicating that high optical quality of millimeter size can be derived by this method. The extinction peaks at ≈1200, 1050, and 940 nm, are not the Bragg diffraction; in the 1 μm particle's periodicity, the Bragg diffraction at the L-point should be observed around at 2.3 μm.

Miyazaki et al. have calculated of the particle-assembled-type photonic crystal [25]. The calculation for an isolated sphere

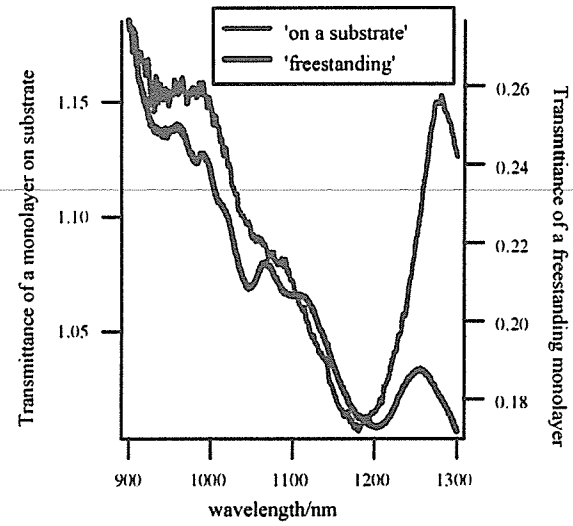

Fig. 5. The experimental results of the transmission spectra of a freestanding monolayer (black line) and of a monolayer on substrate (gray line).

of refractive index $n = 1.6$ with a diameter of 1 μm shows two marked whispering gallery (WG)-mode resonances of $l = 2$ and 3 at 1237 nm and 940 nm, respectively. In our system, we can confirm the extinction peaks that are related to the WG modes at 1180 and 930 nm in the spectrum of the 2D particle array on the substrate, and at 1204 and 940 nm in the spectrum of the freestanding 2D particle array. The spectrum of the freestanding 2D particle array is smoother than that of the 2D particle array on the substrate, and agrees with the theoretical result with respect to the peak positions.

Apart from these WG modes, other extinction peaks are observed at 980 and 1046 nm in a freestanding monolayer. It was calculated that near-field resonance between particles should be observed at 995 and 1014 nm. Now we believe that we can observe the near-field resonance caused by particle alignment without any inhibition from substrates, using freestanding monolayers [26].

4. Conclusions

We show there the freestanding monolayers of 2D particle arrays are prepared by sintering at grass transition temperature. Partially adhesion between particles could be achieved by sintering around grass transition temperature. Freestanding 2D arrays thus prepared became thinner than original film thickness and maintained their original periodicity. This freestanding 2D array would develop its applications not only as a photonic crystal but also as a membrane filter and a culture matrice [27].

Acknowledgments

The present work has been partially supported by the Ministry of Education, Culture, Sorts, Science and Technology, Special postdoctoral research project in RIKEN, and Yazaki Memorial Foundation for Science & Technology.

References

[1] N.D. Denkov, O.D. Velev, P.A. Kralchevsky, I.B. Ivanov, H. Yoshimura, K. Nagayama, Nature 361 (1993) 26.
[2] G. Picard, Langmuir 14 (1998) 3710.
[3] C.D. Dushkin, G.S. Lazarov, S.N. Kotsev, H. Yoshimura, K. Nagayama, Colloid Polym. Sci. 277 (1998) 914.
[4] S. Okuyama, S.I. Matsushita, A. Fujishima, Chem. Lett. (2000) 534.
[5] S.I. Matsushita, T. Miwa, D.A. Tryk, A. Fujishima, Langmuir 14 (1998) 6441.
[6] S. Matsushita, T. Miwa, A. Fujishima, Chem. Lett. (1997) 925.
[7] K. Nagayama, S. Takeda, S. Endo, H. Yohimura, Jpn. J. Appl. Phys. 34 (1995) 3947.
[8] I. Yamashita, Thin Solid Films 393 (2001) 12.
[9] S. Hayashi, I. Kaneko, N. Hojo, Poly. J. 6 (1974) 33.
[10] R. Micheletto, H. Fukuda, M. Ohtsu, Langmuir 11 (1995) 3333.
[11] K. Ohtaka, Phys. Rev. B 19 (1979) 5057.
[12] H. Miyazaki, K. Ohtaka, Phys. Rev. B 58 (1998) 6920.
[13] R. Shimada, A. Imada, T. Koda, T. Fujimura, K. Edamatsu, T. Itoh, K. Ohtaka, K. Takeda, Mol. Cryst. Liq. Cryst. 37 (1999) 95.
[14] P.A. Kralchevsky, K. Nagayama, Langmuir 10 (1994) 23.
[15] H.T. Miyazaki, H. Miyazaki, K. Ohtaka, T. Sato, J. Appl. Phys. 87 (2000) 7152.
[16] S.I. Matsushita, T. Miwa, A. Fujishima, Langmuir 17 (2001) 988.
[17] S.I. Matsushita, Y. Yagi, T. Miwa, D.A. Tryk, T. Koda, A. Fujishima, Langmuir 16 (2000) 636.
[18] Y. Yagi, S.I. Matsushita, D.A. Tryk, T. Koda, A. Fujishima, Langmuir 16 (2000) 1180.
[19] Z. Tadmor, C.G. Gogos, Principles of Polymer Processing, John Wiley & Sons, New York, Chichester, Brisbane, Toronto, Singapore, 1979.
[20] F. Parhami, R.M. McMeeking, A.C.F. Cocks, Z. Suo, Mech. Mat. 31 (1999) 43.
[21] T. Yamasaki, T. Tsutsui, Jpn. J. Appl. Phys. 38 (1999) 5916.
[22] N.D. Denkov, O.D. Velev, P.A. Kralchevsky, I.B. Ivanov, H. Yoshimura, K. Nagayama, Langmuir 8 (1992) 3183.
[23] S. Matsushita, T. Miwa, A. Fujishima, Langmuir 13 (1997) 2582.
[24] P.R. Hornsby, A.S. Maxwell, J. Mat. Sci. 27 (1992) 2525.
[25] H. Miyazaki, K. Ohtaka, Phys. Rev. B 58 (1998) 6920.
[26] S.I. Matsushita, M. Shimomura, Chem. Comm. (2004) 506.
[27] T. Nishikawa, R. Ookura, J. Nishida, K. Arai, J. Hayashi, N. Kurono, T. Sawadaishi, M. Hara, M. Shimomura, Langmuir 18 (2002) 5734.

Available online at www.sciencedirect.com
SCIENCE DIRECT
ELSEVIER
Colloids and Surfaces A: Physicochem. Eng. Aspects 284–285 (2006) 355–358
COLLOIDS AND SURFACES A
www.elsevier.com/locate/colsurfa

Fabrication of luminescent polymeric nanoparticles doped with a lanthanide complex by self-organization process

K. Tamaki [a], H. Yabu [a,b], T. Isoshima [a], M. Hara [a,c], M. Shimomura [a,b,d,*]

[a] *Frontier Research System (FRS), RIKEN, 2-1, Hirosawa, Wako 351-0198, Japan*
[b] *Nanotechnology Research Center, Research Institute for Electronic Science (RIES), Hokkaido University, N21W10, Kita-ku, Sapporo 001-0021, Japan*
[c] *Department of Electronic Chemistry, Interdisciplinary Graduate School of Science and Engineering, Tokyo Institute of Technology, 4259, Nagatsuta-cho, Midori-ku, Yokohama 226-8502, Japan*
[d] *Core Research for Evolutional Science and Technology (CREST), Japan Science and Technology Agency (JST), 4-1-8, Honcho, Kawaguchi 332-0012, Japan*

Received 1 November 2005; received in revised form 29 November 2005; accepted 1 December 2005
Available online 19 January 2006

Abstract

Recently, a simple method for preparation of polymeric particles with narrow size distribution, "self-organized particle precipitation method", has been developed. This method is composed of two steps: firstly a solution of a matrix polymer in a volatile solvent is gradually diluted with a freely miscible poor solvent; then the volatile solvent is gradually evaporated from the mixture. In this work, we report preparation of luminescent polystyrene nanoparticles with narrow size distribution from THF solution of polystyrene and trivalent europium, terbium, and samarium complexes as lumophores. Compared with the polystyrene nanoparticles doped with a lanthanide complex possessing no phenyl group, the polystyrene nanoparticles doped with a complex possessing phenyl groups were highly and uniformly luminescent under ultraviolet light irradiation.

Keywords: Nanoparticles; Self-organization process; Lanthanide complexes; Luminescence

Not only in natural environment but also in our artificial daily life, many kinds of patterns on various scales are spontaneously formed by self-organization processes based on thermodynamically non-equilibrium phenomena [1]. These pattern formation processes are independent on substances composing the patterns. Thus, this pattern formation strategy is applicable to fabrication of novel functional materials. We have already reported that Karman vortices are formed in a droplet of organic polymer solution on a glass substrate [2]. Using this non-equilibrium phenomenon, novel honeycomb-patterned microporous films of various polymers have been fabricated by casting dilute hydrophobic solution of the polymers on a substrate and applying humid air to the solution [3–13]. This film fabrication process is composed of the following steps: water microdroplets, are formed on the surface of the casted polymer solution through condensation from humid air due to cooling by vaporization of the organic solvent; then the water microdroplets grow forming hexagonal arrays without fusing each other, until evaporating all the organic solvent; finally the water microdroplets vaporize from the film, leaving the polymer in a honeycomb pattern.

Recently, we have also established a new pattern formation process using self-organization: fabrication of nanometer- or micrometer-sized polymeric particles with a narrow size distribution. Fabrication of nanoparticles is attracting a lot of attentions in many research and industrial fields, and various fabrication methods have been already reported. Compared with those reported methods, our method has a feature to utilize precipitation for easy and rapid fabrication of nanoparticles, by gradual dilution of organic solution of a polymer with a poor solvent [14,15]. Furthermore, we reported preparation of wrinkled polystyrene (PSt) nanoparticles containing europium or terbium trivalent ion complexes by dispersion free-radical copolymerization of styrene, the lanthanide complex monomer, and hydrophilic macromonomer in polar media [16,17]. The nanoparticles containing europium and terbium complexes emitted red and green luminescence, respectively, with narrow spectral widths of <10 nm as FWHM. Therefore, it can be expected that, by applying our self-organized particle

* Corresponding author.
E-mail address: shimo@poly.es.hokudai.ac.jp (M. Shimomura).

0927-7757/$ – see front matter © 2005 Elsevier B.V. All rights reserved.
doi:10.1016/j.colsurfa.2005.12.003

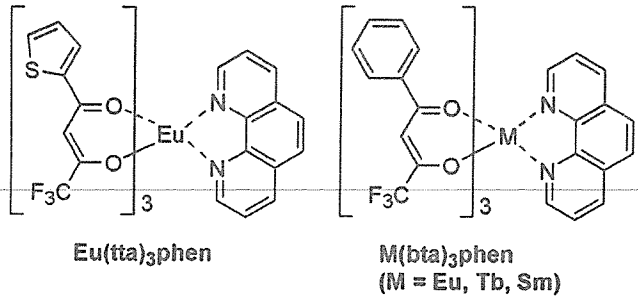

Fig. 1. Chemical structures of lanthanide complexes for dopant.

precipitation to preparation of lanthanide-containing polymeric particles, new polymeric particles with narrow size distribution, controllable surface morphologies, and various dopants as the lumophore will be obtained easily. In this paper, we report fabrication of PSt or poly(methyl methacrylate) (PMMA) nanoparticles doped with europium, terbium, or samarium trivalent ion complexes by the self-organized particle precipitation.

Chemical structures of the compounds used in this work are indicated in Fig. 1. All luminescent lanthanide complexes are known (CAS Registry No. $Eu(tta)_3phen$: 17904-86-8 [18]; $Eu(bta)_3phen$: 31869-48-4 [18]; $Tb(bta)_3phen$: 100294-77-7 [19]; $Sm(bta)_3phen$: 100226-93-5 [20]), and they were synthesized according to a general method [21]. The matrix polymers for particle preparation, PSt (weight-average molecular weight $M_w = 2000000$ and number-average molecular weight $M_n = 1827000$) and PMMA ($M_w = 2\,132000$ and $M_n = 1973000$), were purchased from Sigma-Aldrich and Scientific Polymer Products, respectively. Before using these polymers, they were purified by reprecipitation from mixture of toluene and methanol. Tetrahydrofuran (THF) was purchased from Junsei Chemical and used without further purification.

To obtain lanthanide-doped luminescent polymeric nanoparticles, miscibility of the lanthanide complex to the matrix polymer is very important. Therefore, PSt and PMMA particles doped with $Eu(tta)_3phen$ and $Eu(bta)_3phen$ were fabricated as below. The matrix polymer for nanoparticles (concentration of PSt was 0.267 g/L, and that of PMMA 0.089 g/L) and the dopant lanthanide complex (5.0 or 10.0 wt.% to the matrix polymer) were dissolved in THF. Purified water (Millipore) was gradually added to the solution up to the volume ratio of 1/1, and then THF was gradually evaporated from the aqueous mixture.

The fabricated lanthanide-complex-doped polymer particles were observed by a scanning electron microscope (SEM, Hitachi S-5200). Size distribution of the particles was estimated from SEM images. Emission spectra of the particles were measured by a fluorescence spectrometer (JASCO FP-6500) and microscopic spectroscopy technique using a fluorescence microscope (Olympus IX-70) combined with a high sensitivity spectrophotometer (Horiba Jobin Yvon TRIAX 320/SPECTRUM-1).

Fluorescent microscopic images of particles of the polymer doped with the europium complex (dopant concentration of 5.0 wt.% to the matrix polymer) are indicated in Fig. 2, together with microscopic optical transmission images of the same samples. While not all particles of PSt doped with $Eu(tta)_3phen$ and PMMA doped with $Eu(tta)_3phen$ and $Eu(bta)_3phen$ were luminescent under 330–385 nm UV irradiation, almost all PSt particles doped with $Eu(bta)_3phen$ were luminescent. That is, in the former three combinations of the dopant complexes and matrix polymers, luminescence was highly inhomogeneous among particles, suggesting significant non-uniformity in the dopant concentration.

Luminescence spectra of the europium-complex-doped polymer particles (concentration of 10.0 wt.% to the matrix polymer) are indicated in Fig. 3(b) and (c). While dilute benzene solution of $Eu(tta)_3phen$ under UV irradiation was more luminescent than that of $Eu(bta)_3phen$ as indicated in Fig. 3(a), luminescence of PSt and PMMA particles doped with $Eu(bta)_3phen$ were higher than luminescence of those doped with $Eu(tta)_3phen$. This result may be explained by two reasons. One is that concentration of $Eu(bta)_3phen$ is larger than that of $Eu(tta)_3phen$. The other is that concentration quenching of $Eu(tta)_3phen$ occurs more effectively than that of $Eu(bta)_3phen$ because of inhomogeneous doping of $Eu(tta)_3phen$ in each particle shown in Fig. 2. Thus, the complex $Eu(tta)_3phen$ may highly concentrate and aggregate into certain particles, and other particles may contain almost no complex.

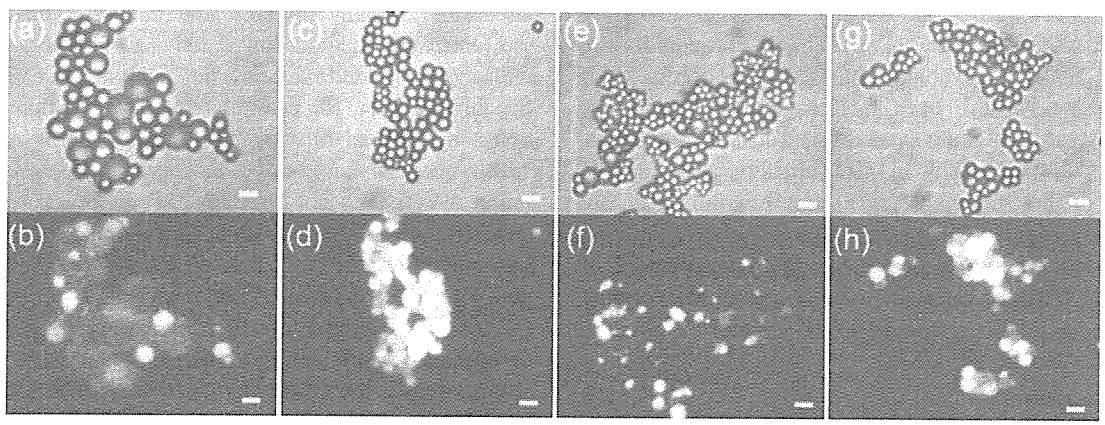

Fig. 2. Microscopic optical transmission (a, c, e, g) and fluorescent microscopic (b, d, f, h) images of particles doped with the europium complexes. (a, b) $Eu(tta)_3phen$ in PSt. (c, d) $Eu(bta)_3phen$ in PSt. (e, f) $Eu(tta)_3phen$ in PMMA. (g, h) $Eu(bta)_3phen$ in PMMA. In the fluorescent microscopic images, the particles were excited at 330–385 nm UV light from a mercury lamp. All scale bars indicate 2.0 μm.